Static and Dynamic Structure Factors for Star Polymers in Θ Conditions

Marina Guenza* and Angelo Perico

Centro di Studi Chimico-Fisici di Macromolecole Sintetiche e Naturali, CNR, Corso Europa 30, 16132 Genova, Italy

Received March 10, 1993

ABSTRACT: The static and dynamic structure factors for star polymers in Θ solutions are derived for semiflexible models and the partially stretched (PS) arm model. The PS model for the static structure factor is found to be in fairly good agreement with SANS experiments with exclusion of the high-k region, where only a qualitative agreement is obtained. The nonpreaveraged first cumulant for the PS model reproduces fairly well the peculiar effects found by neutron spin-echo experiments even though those experiments were carried out in good solvents. The effects of preaveraging and screening of the hydrodynamic interaction are considered. Results for the full dynamic structure factor are presented only in the preaveraging approximation.

Introduction

Our recent model for star polymers in Θ solutions was applied to the evaluation of static and dynamic properties such as the shrinking factor for the mean square radius of gyration and the bond relaxation times in paper 1[1] and paper 2[2] of this series. In the model the star polymer is described as a semiflexible chain with partially stretched arms to take into account the segment concentration effect in the star core. The dynamics were derived in the ORZLD (optimized Rouse-Zimm local dynamics) approach,[3,4] which is of great utility for a general treatment of topological effects in a large hierarchy of polymer models. More recently, a reduced description was introduced which uses the symmetry of the regular star to reduce the computation times required for the calculation of the dynamic properties of long-arm stars. Results for the local relaxation times were first presented.[2] This reduced description is applied in this paper to the calculation of the static and dynamic structure factors of the partially stretched model.

Extensive experimental results[5-9] obtained by SANS and neutron spin-echo experiments were presented for these structure factors, showing interesting peculiar effects due to the star topology such as the emergence of a maximum in the Kratky plot for the static structure factor and a related minimum in the normalized first cumulant plot. These effects are only partially accounted by the classic Gaussian theory.[10,11] Better agreement was achieved by RIS Monte Carlo simulations[5] taking into account both the detailed structure of the polymer and the structure of the star center and by wormlike models with and without specific star centers.[6] Evidence comes out of the relevance of the stretching in the arm interior part. In this paper, we will take into account both semiflexible arms and stretching to derive models for the static structure factor and the dynamic structure factor with its cumulant to explain the peculiar topological experimental effects.

Structure Factors for a Regular Star

Consider a regular star of f arms, each with N bonds of length l and a total number of beads n

$$n = Nf + 1 \tag{1}$$

The position of the ith bead at time t is $R_i(t)$. The beads are conventionally ordered as $i = 1$ for the star center and $i = 2, ..., N+1; N+2, ..., 2N+1; ...; Nf+1$ for the sequence of f arms.

We first introduce the dynamic structure factor expression in the ORZLD approximation. Then we will consider the nonpreaveraged generalized Gaussian case.

The dynamic structure factor is defined, taking into account the Gaussian nature of the random forces in the fluid, as

$$S(k,t) = n^{-2} \sum_{i,j}^{n} \exp\{-(k^2/6)\langle|\mathbf{R}_i(t) - \mathbf{R}_j(0)|^2\rangle\}$$
$$= \exp(-k^2Dt)\, S_I(k,t) \tag{2}$$

with the second equation obtained after separation of the center of mass motion, D the translational diffusion constant, and

$$S_I(k,t) = n^{-2} \sum_{i,j}^{n} \exp\{-(k^2l^2/6)d_{ij}^2(t)\} \tag{3}$$

depending on the relative adimensional intramolecular dynamic distances $d_{ij}^2(t)$. The S_I part can be written for a regular star in the computationally convenient form

$$S_I(k,t) = n^{-2}\{E_{11}(k,t) + f[S_s(k,t) + (f-1)S_c(k,t)]\} \tag{4}$$

with the self term

$$S_s(k,t) = 2\sum_{i=2}^{N+1} E_{1i}(k,t) + \sum_{i=2}^{N+1} E_{ii}(k,t) + 2\sum_{i=2}^{N}\sum_{j=i+1}^{N+1} E_{ij}(k,t) \tag{5}$$

relative to the same arm and the cross term

$$S_c(k,t) = \sum_{i=2}^{N+1} E_{i+N,i}(k,t) + 2\sum_{i=2}^{N}\sum_{j=i+1}^{N+1} E_{i+N,j}(k,t) \tag{6}$$

relative to different arms. The E_{ij} quantity is defined as

$$E_{ij}(k,t) = \exp\{-(k^2l^2/6)d_{ij}^2(t)\} \tag{7}$$

The calculation of S_s only requires a total of $2N + N(N-1)/2$ dynamic distances on the same arm, and S_c requires $N(N+1)/2$ distances between two arms, thus optimizing

0024-9297/93/2226-4196$04.00/0

the computation time. The intramolecular dynamic distances $d_{ij}^2(t)$ are calculated in the ORLZD bead model as[12]

$$d_{ij}^2(t) = \sum_{a=1}^{n-1}[(Q'_{ia})^2 + (Q'_{ja})^2](\mu'_a)^{-1} - 2\sum_{a=1}^{n-1} Q'_{ia}Q'_{ja}(\mu'_a)^{-1}\exp(-\sigma\lambda_a t) \quad (8)$$

with λ_a and Q'_{ia} the eigenvalues and eigenvectors of the product matrix HA and $\mu'_a = ((Q')^T AQ')_{aa}$. The matrix H, defined as

$$H_{ij} = \delta_{ij} + \zeta_r\langle l/R_{ij}\rangle(1-\delta_{ij}) \quad (9)$$

is the matrix of the preaveraged hydrodynamic interactions, while A is the star structural matrix described elsewhere.[1] The bond rate constant σ is given as

$$\sigma = 3k_BT/l^2\zeta \quad (10)$$

with ζ the bead friction coefficient and

$$\zeta_r = \zeta/6\pi\eta_0 l \quad (11)$$

the reduced friction coefficient with η_0 the solvent viscosity. The important first cumulant relative to $S(k,t)$

$$\Omega(k) = -(d/dt)\ln\frac{S(k,t)}{S(k,0)}\Big|_{t=0} \quad (12)$$

using eqs 8 and 9 and the properties of λ_a and μ'_a takes the ORLZD form

$$\Omega(k)/\sigma = (k^2l^2/3n)[S(k,0)]^{-1} \times \{1 + (\zeta_r/n)\sum_{i,j}(1-\delta_{ij})\langle l/R_{ij}\rangle \exp[-(k^2l^2/6)d_{ij}^2(0)]\} \quad (13)$$

For a regular star, eq 13 can be written as in the case of $S(k,t)$ in the computationally covenient form

$$\Omega(k)/\sigma = (k^2l^2/3n)[S(k,0)]^{-1}\{1 + (\zeta_r/n)f[B_s(k) + (f-1)B_c(k)]\} \quad (14)$$

with B_s and B_c the contributions from one arm and two arms, respectively:

$$B_s(k) = 2\sum_{i=2}^{N+1} F_{1i}(k) + 2\sum_{i=2}^{N}\sum_{j=i+1}^{N+1} F_{ij}(k) \quad (15)$$

$$B_c(k) = \sum_{i=2}^{N+1} F_{i+N,i}(k) + 2\sum_{i=2}^{N}\sum_{j=i+1}^{N+1} F_{i+N,j}(k) \quad (16)$$

and

$$F_{ij}(k) = E_{ij}(k,0)\langle l/R_{ij}\rangle \quad (17)$$

It is noteworthy that in the case of the first cumulant a nonpreaveraged expression is available[13,14] and may be expressed in the general form

$$\Omega(k) = (k_BT/\zeta)\sum_{i,j}\langle(\mathbf{k}\cdot\mathbf{H}_{ij}\cdot\mathbf{k})\exp(i\mathbf{k}\cdot\mathbf{R}_{ij})\rangle/[n^2S(k,0)] \quad (18)$$

The tensor $\mathbf{H}_{ij}$

$$\mathbf{H}_{ij} = 1\delta_{ij} + \zeta(1-\delta_{ij})\mathbf{T}_{ij} \quad (19)$$

describes the nonpreaveraged hydrodynamic interaction with

$$\mathbf{T}_{ij} = (8\pi\eta_0 R_{ij})^{-1}(1 + \mathbf{R}_{ij}\mathbf{R}_{ij}/\mathbf{R}_{ij}^2) \quad (20)$$

the Oseen tensor.

Equation 18 is evaluated[15] by averaging first over the orientations and subsequently over scalar distances using a generalized Gaussian distribution to obtain $\Omega(k)$ correct to second-order moments. The generalized result is

$$\Omega(k)/\sigma = (k^2l^2/3n)[S(k,0)]^{-1}\{1 + (\zeta_r/n)\sum_{i,j}(1-\delta_{ij})\langle l/R_{ij}\rangle(3/4)H(x)\} \quad (21)$$

with

$$H(x) = (x^{-3} + 2x^{-1})\exp(-x^2)\int_0^x \exp(t^2)\,dt - x^{-2} \quad (22)$$

$$x^2 = k^2\langle R_{ij}^2\rangle/6 \quad (23)$$

and $\langle R_{ij}^2\rangle = l^2d_{ij}^2(0)$ the static mean square distances in the chosen model. These equations for the nonpreaveraged first cumulant are not restricted to simple Gaussian chains but, using the proper second moments and $\langle l/R_{ij}\rangle$, describe stiffness as well as solvent effects.

Inspection of eqs 13 and 21 shows that the preaveraging approximation amounts to substituting $(3/4)H(x)$ with $\exp(-x^2)$ independently of the assumed specific generalized Gaussian model.

Following the same procedure of the preaveraging case, eq 21 can be rewritten to obtain an equation identical to (14) with the definition of $F_{ij}(k)$ (eq 17) changed to $F'_{ij}(k)$:

$$F'_{ij}(k) = (3/4)H(x)\langle l/R_{ij}\rangle \quad (17')$$

Finally, the ORLZD result for the translational diffusion constant D takes the Kirkwood form:[16]

$$D = (k_BT/n\zeta)[1 + (\zeta_r/n)\sum_{i\neq j}\langle l/R_{ij}\rangle] \quad (24)$$

It remains to calculate the dynamic and static mean square distances together with the inverse static distances. As in the following we assume for $\langle l/R_{ij}\rangle$ the Gaussian value

$$\langle l/R_{ij}\rangle \approx (6/\pi)^{1/2}(\langle R_{ij}^2\rangle)^{-1/2} \quad (25)$$

we are left with the computation of only the mean square distances.

In this paper star models with semiflexible arms described as freely rotating chains (FRC) or partially stretched freely rotating chains (PS) are considered. Each arm has the first N' ($\leq N$) bonds characterized by a valence angle θ' and the remaining $N - N'$ bonds by a valence angle θ, with

$$p' = -\cos\theta' \quad (26)$$

$$p = -\cos\theta \quad (27)$$

the stiffness of the core and the stiffness of the outer part of the star, respectively ($p' \leq p$). Following paper 1, the correlation of the bond vectors attached to the star center is assumed as

$$\langle \mathbf{l}_1^i\cdot\mathbf{l}_1^j\rangle = \alpha \quad (28)$$

for any two different arms, with $\mathbf{l}_1^i$ the first bond of arm i. In this paper α is assumed to take its minimum value $-(f-1)^{-1}$, with the exclusion of the Gaussian case where $\alpha = 0$.

For polystyrene in Θ solutions[1] a value of $p = 0.77$ was determined from the experimental radius of gyration of linear polymers, while values of $p' = 0.87$ and $N' = 250$ were obtained by fitting the experimental molecular weight dependence of the shrinking ratio.

$$g = \langle S^2\rangle_{star}/\langle S^2\rangle_{linear} \quad (29)$$

The static distances for the FRC and PS models are calculated by a straightforward procedure outlined in the

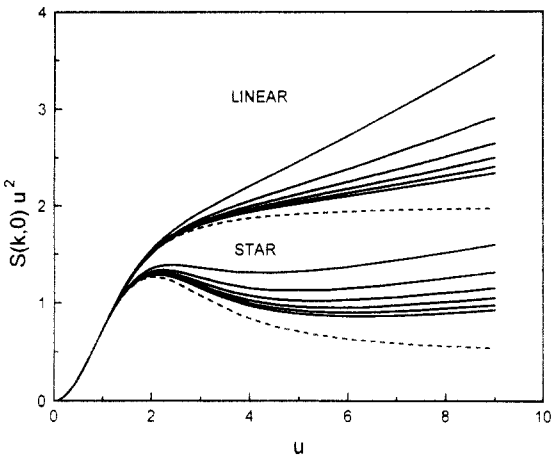

Figure 1. Kratky plot for the static structure factor $S(k,0)u^2$ against u, $u = k(\langle S^2 \rangle)^{1/2}$ for semiflexible FRC models ($p = 0.77$). Regular star polymers ($f = 12$): lower curves. Linear polymers at the same molecular weight: upper curves. The curves decrease with increasing number of beads: $n-1 = 240, 480, 720, 960, 1200$, and 1440. The dashed curves are the two Gaussian limits.

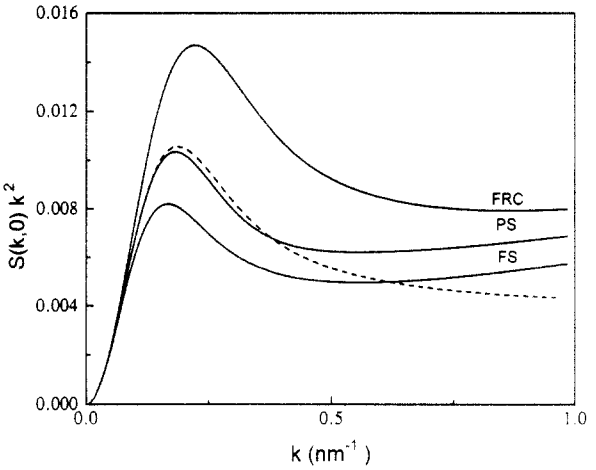

Figure 2. $S(k,0)k^2$ against k for some star models at $M = 467000$, $f = 12$, and $N = 374$. FS: fully stretched arm model with $p = 0.87$. PS: partially stretched arm model with $p = 0.77$, $p' = 0.87$, and $N' = 110$. FRC: fully rotating chain star model at $p = 0.77$. Dashed curve: Gaussian model with an effective bond length of 8.24 Å.

Appendix of paper 1, and the results are reported in Appendix A of the present paper. The calculations of the dynamic distances require more sophisticated considerations and are reported in a special section.

Static Structure Factor

The static structure factor $S(k,0)$ is calculated from eq 3 in the $t \to 0$ limit given the static distances (see Appendix A). Figure 1 reports a Kratky plot ($u = k(\langle S^2 \rangle)^{1/2}$) for FRC linear and star polymers ($f = 12$) at p = 0.77 and different arm lengths N. All the curves display the well-known universal behavior for small u, while for large u the curves for star polymers separate from the linear ones and show a maximum.[10] The curves lower as the molecular weight increases, and in the limit of large N Gaussian behavior is approached for both linear and star polymers.

Figure 2, reports a plot of $S(k,0)k^2$ against k for three models describing polystyrene stars at $M = 467000$. The partially stretched star model gives results fairly different from the simple FRC star ($p = 0.77$) and from the fully stretched arm star (FS: $p = 0.87, N = N'$). On the contrary, when the Gaussian model is fitted to have an effective segment length giving the same radius of gyration as the PS model, the PS curve and the Gaussian curve are similar

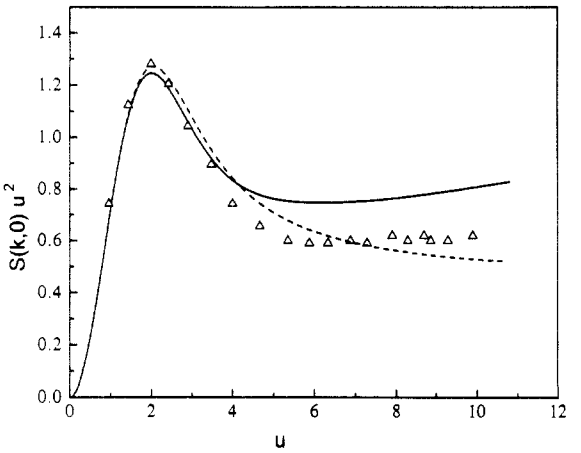

Figure 3. Kratky plot for polystyrene at $M = 467000$. SANS experimental results from Huber et al.:[5] (Δ). PS model: full curve. Gaussian model with an effective segment length of 8.24 Å: dashed curve.

up to $k = 0.4$. For larger k, the PS curve increases regularly with k due to stiffness while the Gaussian curve remains constant. In addition, the PS curve is a bit steeper than the Gaussian curve after the maximum. As the PS curve was calculated using the parameters derived from fitting the experimental molecular weight dependence of the shrinking factor g, it turns out that also the static structure factor is sensitive to these parameters.

Figure 3 reports a Kratky plot for polystyrene at $M = 467000$, where the PS curve is compared to SANS experimental results.[5] In the PS model for this molecular weight, the value N' has been reduced from 250 to 110 to take into account the variance of this experimental point in the g against M curve. Note that N' is a much less sensitive parameter than the stiffness p' in the fitting procedure. The agreement with the experiment is extended up to $u = 4$, which is a good confirmation of the model parameters determined by fitting the shrinking factor.[1] For higher u values the model gives quantitative differences with the experiment but a qualitative agreement with the curve upturn due to stiffness. Clearly, for a better agreement in the limit of extremely large u values one should use a less rough model for the partial stretching of the arms and a more appropriate description of the local stiffness (RIS models).

The First Cumulant

The exact first cumulant $\Omega(k)$ is derived from eq 21 and the static distances of Appendix A. In Figure 4, the results are compared for semiflexible (FRC, $p = 0.77$) and Gaussian models of linear and star polymers. As is well known,[7] in the Gaussian case the topological structure of the star implies the emergence of a minimum in the intermediate region between the diffusion-like behavior (low u) and the Zimm behavior (high u). In the case of semiflexible chains we have a smooth minimum even in the linear case. In addition, linear and star curves do not match at high u values. Globally, $\Omega(k)$ increases with stiffness, and the minimum, characterizing the star topology, becomes deeper.

The question of the width and depth of the topological minimum is better analyzed in Figure 5, where model results for polystyrene at $M = 467000$ are presented. Defining as depth d of the minimum the difference between the values of normalized $\Omega(k)/k^3$ at the minimum and at the smooth maximum in the high-u region and as width Δu the value at half the depth, we find for the PS model $d = 45\%$ of the smooth maximum and $\Delta u = 3.36$. In the

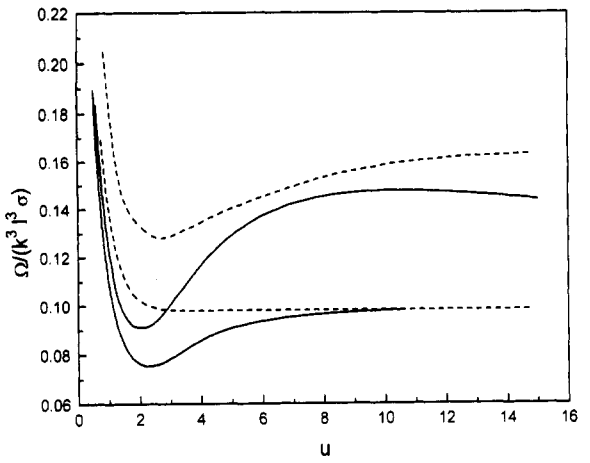

Figure 4. Exact normalized adimensional first cumulant $\Omega(k)/[\sigma k^3 l^3]$ against u for linear (dashed curve) and star polymers (f = 12; full curves) at the same molecular weight $n - 1 = 1440$. Upper curves: FRC models at $p = 0.77$. Lower curves: Gaussian models ($p = 0$).

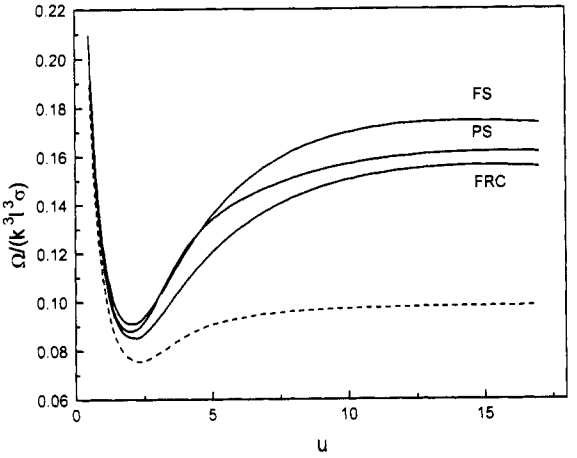

Figure 5. Exact first cumulant $\Omega(k)/[\sigma k^3 l^3]$ against u for N = 374 and f = 12. FS, PS, and FRC same as in Figure 2. Dashed curve: Gaussian model ($p = 0$).

case of Gaussian stars we get smaller values: $d = 22\%$ and $\Delta u = 2.85$. It is interesting to note that the FRC star gives $d = 45\%$ and $\Delta u = 3.95$ for the nonstretched model (p = 0.77) and $d = 48\%$ and $\Delta u = 3.90$ for the totally stretched model (p = 0.87). This implies that the minimum is enhanced by stiffness and stretching. It is noteworthy that these PS values are comparable with the results obtained by neutron spin–echo experiments on polyisoprene in good solvents obtained by Richter et al.[7] (the width there is given as $\Delta v = (f/(3f-2)^{1/2})\Delta u$). In addition, Richter et al.[7] suggest that in star polymers the screening of the hydrodynamic interaction due to the high segment concentration in the interior of the star should cause an enhancement of the minimum.

In Figure 6 we address this point, comparing results for PS models at two values of the hydrodynamic interaction strength ζ_r. As ζ_r decreases from 0.25, typical of linear chains in Θ conditions, to 0.20, the curve for normalized $\Omega(k)/k^3$ becomes lower and the depth increases from 45% to 49%, while the width increases from 3.36 to 3.52. This is a confirmation that a dynamic model for star polymers should take into account some screening (increasing with f) of the hydrodynamic interaction due to the high concentration of segments in the core of the star.

The Dynamic Distances

The ORZLD dynamic distances, given in eq 8 in terms of normal modes in the bead description, are written now

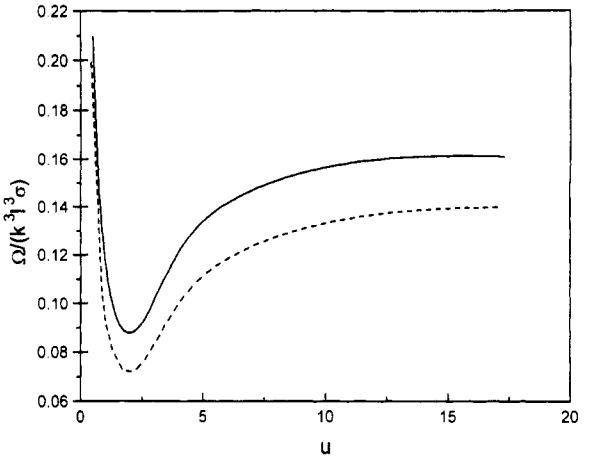

Figure 6. Effect of the hydrodynamic interaction on the exact first cumulant: $N = 374$, $f = 12$, PS model. Full curve: $\zeta_r = 0.25$. Dashed curve: $\zeta_r = 0.20$.

in the reduced bond description of paper 2. The reduced bond description is of great utility, as it reduces the order of matrices to be diagonalized from n to N, saving an enormous quantity of computing time, thus allowing one to treat higher molecular weights. First, we introduce the definitions of bead normal modes

$$\mathbf{R}_i(t) = \sum_{a=0}^{n-1} Q'_{ia}\xi'_a(t) \tag{30}$$

and bond normal modes

$$\mathbf{l}_i(t) = \sum_{a=1}^{n-1} Q_{ia}\xi_a(t) \tag{31}$$

The bead coordinates are related to the bond coordinates by the equation

$$\begin{aligned}\mathbf{R}_i(t) &= \sum_{j=0}^{n-1} M_{ij}^{-1}\mathbf{l}_j(t) \\ &= \mathbf{l}_0(t) + \sum_{j=i}^{n-1} M_{ij}^{-1}\mathbf{l}_j(t)\end{aligned} \tag{32}$$

Here, $\mathbf{l}_0$ is the coordinate of the center of mass:

$$\begin{aligned}\mathbf{l}_0(t) = \mathbf{R}_{cM}(t) &= n^{-1}\sum_{i=0}^{n-1}\mathbf{R}_i(t) \\ &= \mathbf{R}_r(t) + \Delta\end{aligned} \tag{33}$$

with Δ the difference between the center of mass $\mathbf{R}_{cM}(t)$ and the center of resistance $\mathbf{R}_r(t)$. The bead-to-bond transformation matrix M and its inverse M^{-1} for a regular star were given in paper 2 as eqs 11 and 58.

The eigenvectors Q' are related to the Q by the equation

$$Q'_{ia} = \sum_{j=0}^{n-1} M_{ij}^{-1}Q^c_{ja} \tag{34}$$

with

$$Q^c = \begin{pmatrix} n^{-1/2} & n^{-1}\sum_{i=0}^{n-1}Q'_{i1} & n^{-1}\sum_{i=0}^{n-1}Q'_{i2} & \cdots \\ 0 & & & \\ 0 & & Q & \end{pmatrix} \tag{35}$$

after a proper normalization of Q.

With these definitions the dynamic distances, decoupling explicitly the mode relative to the center of resistance

to the other modes, take the form

$$\langle|\mathbf{R}_i(t) - \mathbf{R}_j(0)|^2\rangle = 6Dt + l^2 d_{ij}^2(t) = 6Dt + \epsilon_{ij}(t) + l^2 b_{ij}^2(t) \quad (36)$$

and

$$\epsilon_{ij}(t) = \langle|\Delta(t) - \Delta(0)|^2\rangle + 2\langle(\Delta(t) - \Delta(0)) \times [\sum_{k=1}^{n-1} M_{ik}^{-1}\mathbf{l}_k(t) - \sum_{k=1}^{n-1} M_{jk}^{-1}\mathbf{l}_k(0)]\rangle \quad (37)$$

is the correction to the bond dynamic distances:

$$l^2 b_{ij}^2(t) = \langle|\sum_{k=1}^{n-1} M_{ik}^{-1}\mathbf{l}_k(t) - \sum_{k=1}^{n-1} M_{jk}^{-1}\mathbf{l}_k(0)|^2\rangle \quad (38)$$

The difference Δ, given in terms of bead modes as

$$\Delta(t) = \sum_{a=1}^{n-1} d_a \xi'_a(t) \quad (39)$$

turns out to be zero only in the free-draining case, where the coefficients d_a, defined as

$$d_a = n^{-1} \sum_{m=0}^{n-1} Q'_{ma} \quad (40)$$

become identically zero. The term $\epsilon_{ij}(t)$ becomes zero with Δ and is a small contribution, easy to calculate in the bead mode description but highly computer time consuming in the bond description because it requires the solution of eq 34 with Q' satisfying normalization conditions and the relation

$$\sum_a (Q'^{-1})_{ai} = n^{1/2}\delta_{i0} \quad (41)$$

Therefore we shall evaluate ϵ_{ij} only in the bead mode description to estimate its relative contribution to the exact dynamic distances. Taking into account that

$$\mathbf{l}_k(t) = \sum_{a=1}^{n-1} Q^c_{ka} \xi'_a(t) \quad (42)$$

and the properties of the bead normal modes, we get the final bead mode expression for the correction term:

$$\epsilon_{ij}(t) = 2\sum_{a=1}^{n-1} d_a[1 - \exp(-\sigma\lambda_a t)](\mu'_a)^{-1}[Q'_{ia} + Q'_{ja} - d_a] \quad (43)$$

with the contribution quadratic in Δ given by

$$\langle|\Delta(t) - \Delta(0)|^2\rangle = 2\sum_{a=1}^{n-1} d_a^2[1 - \exp(-\sigma\lambda_a t)](\mu'_a)^{-1} \quad (44)$$

We can now proceed to an estimation of the relative importance of the terms $\epsilon_{ij}(t)$ in comparison to the full $d_{ij}^2(t)$ terms. For all models, the second term in eq 37 gives the largest contribution. From expression 43 it turns out that the maximum value of $\epsilon_{ij}(t)$ is obtained in the long-time limit. The relative importance, $\epsilon_{ij}(t)/d_{ij}^2(t)$, is greater for the dynamic distances with $i = j$, the maximum contribution coming from the small i values of the star core. In the case of Gaussian chains with $f = 12$ and $N = 10$, the $i = j = 1$ term contributes as much as 20%, while for other distances the contribution is greatly lower. In addition, for increasing stiffness, the role of these terms decreases.

In the next section we will check the contribution of $\epsilon_{ij}(t)$ to $S(k,t)$ for small N and to the first cumulant $\Omega(k)$ for higher N.

In Appendix B, the bond dynamics terms $b_{ij}^2(t)$ are calculated taking into account the symmetry properties of M^{-1} and the properties and symmetry of the bond modes according to paper 2. The result can be summarized in terms of degenerate and nondegenerate eigenvalues and eigenvectors of the regular star as

$$b_{ij}^2(t) = \langle r_{1i}^2\rangle/l^2 + \langle r_{1j}^2\rangle/l^2 - 2\langle\mathbf{r}_{1i}(t)\cdot\mathbf{r}_{1j}(0)\rangle/l^2 + 2f\sum_{a=1}^{N} C_a^2(\mu_a^N)^{-1}\{1 - \exp(-\sigma\lambda_a^N t)\} - 2\sum_{a=1}^{N} C_a(E_{ai} + E_{aj})(\mu_a^N)^{-1}\{1 - \exp(-\sigma\lambda_a^N t)\} \quad (45)$$

with

$$\langle\mathbf{r}_{1i}(t)\cdot\mathbf{r}_{1j}(0)\rangle/l^2 = (f-1)f^{-1}\sum_{a=1}^{N} D_{ai}D_{aj}(\mu_a^D)^{-1} \times \exp(-\sigma\lambda_a^D t) + f^{-1}\sum_{a=1}^{N} E_{ai}E_{aj}(\mu_a^N)^{-1}\exp(-\sigma\lambda_a^N t) \quad (46)$$

for i and j on the same arm, and

$$\langle\mathbf{r}_{1i}(t)\cdot\mathbf{r}_{1j}(0)\rangle/l^2 = -f^{-1}\sum_{a=1}^{N} D_{ai}D_{aj}(\mu_a^D)^{-1}\exp(-\sigma\lambda_a^D t) + f^{-1}\sum_{a=1}^{N} E_{ai}E_{aj}(\mu_a^N)^{-1}\exp(-\sigma\lambda_a^N t) \quad (46')$$

on different arms. $\langle r_{1i}^2\rangle l^2$ is the mean square distance of bead i to the center of the star given in Appendix A. The coefficients C_a, E_{ai}, and D_{ai} are defined as

$$C_a = n^{-1}\sum_{k}^{N} (N - k + 1)Q_{ka}^N \quad (47)$$

$$E_{ai} = \sum_{m=1}^{i-1} Q_{ma}^N \quad (48)$$

$$D_{ai} = \sum_{m=1}^{i-1} Q_{ma}^D \quad (49)$$

Note that here $\{\lambda_a^D, \lambda_a^N\}$, $\{Q^D, Q^N\}$, and $\{\mu_a^D, \mu_a^N\}$ are the degenerate and nondegenerate eigenvalues, eigenvectors, and diagonal elements describing the inverse of the mean square lengths of the modes, given in paper 2.

The Dynamic Structure Factor

The full dynamic structure factor $S(k,t)$ can be computed in the preaveraging approximation by directly using eq 2 with the exact preaveraged dynamic distances of eq 8. This procedure, however, is impractical for high n due to the large dimensions of the matrices to diagonalize. On the other hand, the use of the reduced description requires one to approximate the dynamic distance d_{ij}^2 with the bond mode contribution $b_{ij}^2(t)$. This approximation can be evaluated directly for small N: a typical result is reported in Figure 7 for the FRC star at $p = 0.77$, $f = 12$, and $N = 10$. It can be seen that the approximation is fairly good. For higher N values an estimation of this approximation can be obtained by studying the preaveraged first cumulant. Taking into account that from (36)

$$b_{ij}^2(t) = d_{ij}^2(t) - \epsilon_{ij}(t) \quad (50)$$

we can derive from (8) and (43) the relationship between the preaveraged $\Omega(k)$ calculated using the bond distances

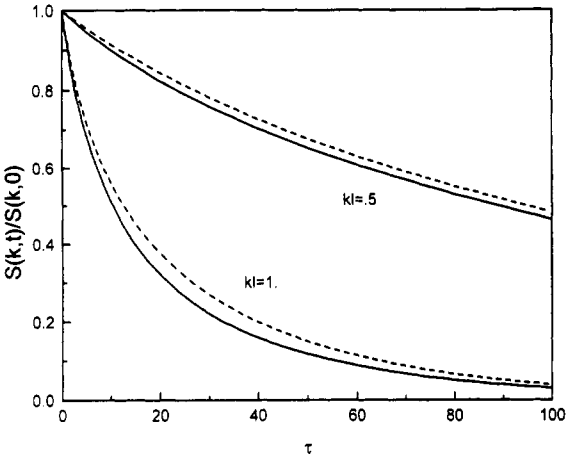

Figure 7. Normalized preaveraged dynamic structure factor as a function of the adimensional time $\tau = \sigma t$ for the FRC star model with $f = 12$, $N = 10$, and $p = 0.77$ at different kl. Full curves: exact preaveraged dynamic distances in the bead description. Dashed curves: approximate dynamic distances in the bond description.

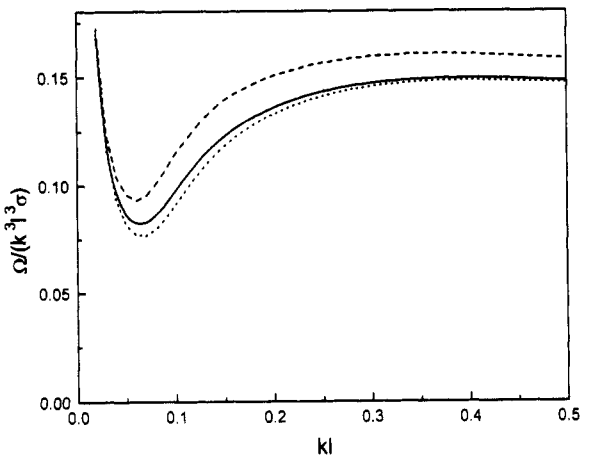

Figure 8. Normalized adimensional first cumulant against kl for PS models at $f = 12$, $N = 374$, $p = 0.77$, $p' = 0.87$, and $N' = 110$. Full curve: preaveraged bead description; dotted curve: preaveraged bond description; dashed curve: nonpreaveraged exact result.

and the exact bead distances:

$$(\Omega(k)/\sigma)_{\text{bond}} = \Omega(k)/\sigma + (2/3)(k^2l^2/n^2)\zeta_\tau \sum_{i,j} \{(1-\delta_{ij}) \times \langle l/R_{ij}\rangle - n^{-1}[\sum_{m\neq i}\langle l/R_{mi}\rangle][S(k,0)]^{-1} \exp[-(k^2l^2/6)d_{ij}^2(0)]\} \quad (51)$$

The computation of the exact preaveraged $\Omega(k)$ and of eq 51 requires only the static distances given in Appendix A and therefore can be performed up to high N values.

Figure 8 reports the comparison of approximate and exact preaveraged $\Omega(k)$ for the PS model. The differences are very small with their maximum at the minimum, where a difference up to 7% is found.

In the same figure, the exact nonpreaveraged result is also reported to show the well-known[15] large effect of preaveraging. In comparison to the preaveraging, the error due to the use of bond distances is minor. Therefore in the remainder of this section we will discuss, as a first guess to the exact dynamic structure factor, its preaveraged form, as computed using the reduced bond distances.

Figure 9 reports a plot of $\ln[S(k,t)/S(k,0)]$ against $\Omega(k)t$ at several values of kl for the PS star. The general behavior of this plot is similar to that reported for linear chains.[14] As time increases, the slope increases from the value −1, which characterizes the short-time behavior. As kl increases, the time range characterized by a slope near −1 extends to larger Ωt values as found in the linear case (for $kl = 10$ the −1 slope is approximately found up to $\Omega t = 7$). Therefore this kind of plot for the dynamic structure factor does not reveal any peculiar qualitative effect due to the polymer architecture.

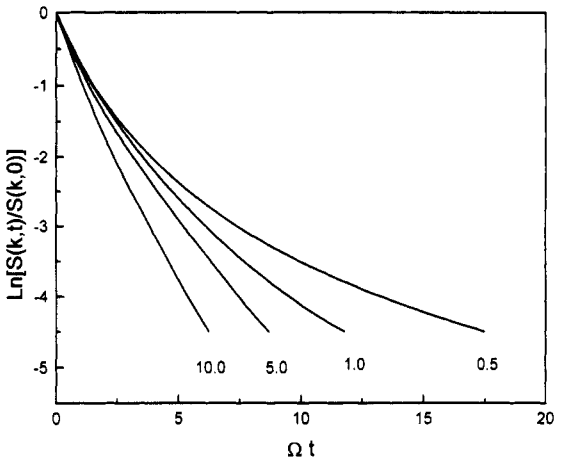

Figure 9. Preaveraged normalized dynamic structure factor calculated in the bond distance approximation against Ωt for $kl = 0.5$, 1, 5, and 10 (from top to bottom). PS model with $f = 12$, $N = 200$, $N' = 100$, $p = 0.77$, and $p' = 0.87$.

Nevertheless, it could be of interest to compare quantitatively these predictions with the experimental behavior in Θ solutions to analyze the role of the preaveraging of the hydrodynamic interaction and of the partially stretched semiflexible star model on the long-time behavior of $S(k,t)$.

Conclusions

We have discussed here the static and dynamic structure factor for a star polymer in Θ solutions. Calculations are presented for semiflexible star models and a partially stretched star model that we already found describe well the experimental shrinking factor behavior with M. In the case of the static structure factor our results can be compared to SANS experiments. The agreement with the partially stretched star model is again fairly good. However, in the high-k region, only a qualitative agreement is obtained, probably due to the rough local details contained in the model. The effect of the preaveraging of the hydrodynamic interaction is considered. For the first cumulant $\Omega(k)$ a direct comparison with experiment is not possible as data in Θ conditions are not available. Nevertheless, the calculated nonpreaveraged $\Omega(k)$ for the partially stretched star model is in qualitative agreement with neutron spin–echo experiments in good solvents. The role of the screening of the hydrodynamic interaction is briefly discussed. In the case of the full dynamic structure factor, results are presented and discussed only in the preaveraging approximation.

Appendix A

In Appendix A of paper 1 the general expressions (eqs A3–A10) of the static distances d_{ij}^2 in terms of static bond vector correlations were given for stars having two regions of different stiffness (FRC and PS stars). As that Appendix did not report the final results, they are reported here as we need them in the computations of $S(k,0)$ and $\Omega(k)$. The results are given for a PS star with an arm length N, a core region of length N' and stiffness p', and an outer region of stiffness p.

For distances on the same arm and in the interior of a region of stiffness p (or p') the result is simply that of a

freely rotating chain of stiffness p (or p')

$$d_{ij}^2 = f_{ij}^2(p) = |i-j|\{(1+p)/(1-p) - (2p/|i-j|)(1-p^{|i-j|})/(1-p)^2\} \quad \text{(A1)}$$

In the case of distances between beads on two different stiffness regions on the same arm, the result is

$$d_{ij}^2 = f_{i,N'+1}^2(p') + f_{N'+1,j}^2(p) + 2pA_j[(p')^{N'+1-i} - 1]/(p'-1) \quad \text{(A2)}$$

$$1 \le i \le N'; \quad N'+2 \le j \le N+1$$

and

$$A_j = [(p)^{j-N'-1} - 1]/(p-1) \quad \text{(A3)}$$

On two different arms we have three cases:
If the beads i and j are both in the core region, then

$$d_{ij}^2 = f_{1i}^2(p') + f_{1j}^2(p') - 2\alpha A'_i A'_j \quad \text{(A4)}$$

$$2 \le i,j \le N'+1$$

and

$$A'_i = [(p')^{i-1} - 1]/(p'-1) \quad \text{(A5)}$$

If i and j are both located in the outer region, then

$$d_{ij}^2 = 2f_{1,N'+1}^2(p') + f_{N'+1,i}^2(p) + f_{N'+1,j}^2(p) + 2p^2BA_i + 2p^2BA_j - 2\alpha\{B^2 + (p')^{N'-1}pB(A_i + A_j) + (p')^{2N'-2}p^2A_iA_j\} \quad \text{(A6)}$$

$$N'+2 \le i,j \le N+1$$

Finally, if i is in the core region and j is in the outer region, then

$$d_{ij}^2 = f_{1i}^2(p') + f_{1,N'+1}^2(p') + f_{N'+1,j}^2(p) + 2pBA_j - 2\alpha\{BA'_i + (p')^{N'-1}pA'_iA_j\} \quad \text{(A7)}$$

$$2 \le i \le N'+1; \quad N'+2 \le j \le N+1$$

with

$$B = [(p')^{N'} - 1]/(p'-1) \quad \text{(A8)}$$

Appendix B: Bond Dynamic Distances

The calculation of the bond contribution to the dynamic distances starts with eq 35:

$$b_{ij}^2(t) = \langle|\sum_{k=1}^{n-1}(M^{-1})_{ik}\mathbf{l}_k(t) - \sum_{k=1}^{n-1}M_{jk}^{-1}\mathbf{l}_k(0)|^2\rangle \quad \text{(B1)}$$

Introducing the definition of M^{-1} for a regular star, given as a block matrix in eq 58 of paper 2, we can separate the vectors included in (B1) into two cases:
for $i = 1$

$$\sum_{k=1}^{n-1}M_{1k}^{-1}\mathbf{l}_k = -\sum_{k=1}^{N}(N-k+1)n^{-1}\sum_{\delta=1}^{f}\mathbf{l}_k^{\delta} \quad \text{(B2)}$$

and for $1 < i \le N$ on the arm γ

$$\sum_{k=1}^{n-1}M_{ik}^{-1}\mathbf{l}_k = \sum_{a=1}^{i-1}\mathbf{l}_a^{\gamma} - \sum_{k=1}^{N}(N-k+1)n^{-1}\sum_{\delta=1}^{f}\mathbf{l}_k^{\delta} \quad \text{(B3)}$$

On the right-hand side of eqs B2 and B3 a superscript δ has been used to identify the arm which the bond vector belongs to. When eqs B2 and B3 are inserted into eq B1, the average is split into terms involving scalar products of the bond vectors of the type $\langle\mathbf{l}_k^{\gamma}(t)\cdot\mathbf{l}_k^{\delta}(0)\rangle/l^2$. Now, introducing the bond modes and the expression for the bond eigenvectors Q, given in terms of degenerate and nondegenerate eigenvectors by eqs 40 and 45 in paper 2, the time correlation between bond vectors is finally obtained as

$$\langle\mathbf{l}_k^{\gamma}(t)\cdot\mathbf{l}_i^{\gamma}(0)\rangle/l^2 = (f-1)f^{-1}\sum_{a=1}^{N}Q_{ka}^{D}Q_{ia}^{D}(\mu_a^{D})^{-1} \times \exp(-\sigma\lambda_a^{D}t) + f^{-1}\sum_{a=1}^{N}Q_{ka}^{N}Q_{ia}^{N}(\mu_a^{N})^{-1}\exp(-\sigma\lambda_a^{N}t) \quad \text{(B4)}$$

for vectors on the same arm γ and

$$\langle\mathbf{l}_k^{\gamma}(t)\cdot\mathbf{l}_i^{\delta}(0)\rangle/l^2 = -f^{-1}\sum_{a=1}^{N}Q_{ka}^{D}Q_{ia}^{D}(\mu_a^{D})^{-1}\exp(-\sigma\lambda_a^{D}t) + f^{-1}\sum_{a=1}^{N}Q_{ka}^{N}Q_{ia}^{N}(\mu_a^{N})^{-1}\exp(-\sigma\lambda_a^{N}t) \quad \text{(B5)}$$

for vectors on different arms. Note that, in the static limit and for the freely rotating star with stiffness p and correlation at the star center α the following summations are obtained:

$$\sum_{a=1}^{N}Q_{ka}^{N}Q_{ia}^{N}(\mu_a^{N})^{-1} = [1 + \alpha p^{2(k-1)}(f-1)]p^{|i-k|} \quad \text{(B6)}$$

$$\sum_{a=1}^{N}Q_{ka}^{D}Q_{ia}^{D}(\mu_a^{D})^{-1} = [1 - \alpha p^{2(k-1)}]p^{|i-k|} \quad \text{(B7)}$$

Using (B4) and (B5) we get the final expression for $b_{ij}^2(t)$ reported in eq 45 as a function of degenerate and nondegenerate eigenvalues and eigenvectors.

References and Notes

(1) Guenza, M.; Mormino, M.; Perico, A. *Macromolecules* **1991**, *24*, 6168 (paper 1).
(2) Guenza, M.; Perico, A. *Macromolecules* **1992**, *25*, 5942 (paper 2).
(3) Perico, A.; Guenza, M. *J. Chem. Phys.* **1985**, *83*, 3103.
(4) Perico, A. *Acc. Chem. Res.* **1989**, *22*, 336.
(5) Huber, K.; Burchard, W.; Bantle, S.; Fetters, L. J. *Polymer* **1987**, *28*, 1997.
(6) Huber, K.; Burchard, W. *Macromolecules* **1989**, *22*, 3332.
(7) Richter, D.; Stuhn, B.; Ewen, B.; Nerges, D. *Phys. Rev. Lett.* **1987**, *58*, 2462.
(8) Richter, D.; Farago, B.; Huang, J. S.; Fetters, L. J.; Ewen, B. *Macromolecules* **1989**, *22*, 468.
(9) Richter, D.; Farago, B.; Fetters, L. J.; Huang, J. S.; Ewen, B. *Macromolecules* **1990**, *23*, 1845.
(10) Burchard, W. *Adv. Polym. Sci.* **1983**, *48*, 1.
(11) Benoit, H. *J. Polym. Sci.* **1953**, *11*, 507.
(12) Perico, A.; La Ferla, R.; Freed, K. F. *J. Chem. Phys.* **1989**, *91*, 4387.
(13) Akcasu, Z.; Gurol, H. *J. Polym. Sci., Polym. Phys. Ed.* **1976**, *14*, 1.
(14) Akcasu, Z.; Benmouna, M.; Han, C. C. *Polymer* **1980**, *21*, 866.
(15) Burchard, W.; Schmidt, M.; Stockmayer, W. H. *Macromolecules* **1980**, *13*, 580.
(16) Kirkwood, J. G. *J. Polym. Sci.* **1954**, *12*, 1.